Title

The influence of compact and ordered carbon coating on solid-state behaviors of silicon during electrochemical processes

Journal

Carbon Energy, 2(1)

ISSN

2637-9368

Authors

Zhou, Shuo
Fang, Chen
Song, Xiangyun
et al.

Publication Date

2020-03-01

DOI

10.1002/cey2.28

Peer reviewed

The influence of compact and ordered carbon coating on solid-state behaviors of silicon during electrochemical processes

Shuo Zhou[+], Chen Fang[+], Xiangyun Song, and Gao Liu*

Energy Storage and Distributed Resources Division, Lawrence Berkeley National Laboratory, Berkeley, California 94720, United States.

*Corresponding author. E-mail: gliu@lbl.gov.

[+]Shuo Zhou and Chen Fang should be considered joint first author.

ABSTRACT

To address the issues of large volume change and low conductivity of silicon (Si) materials, carbon coatings have been widely employed as surface protection agent and conductive medium to encapsulate the silicon materials, which can improve the electrochemical performance of Si-based electrodes. There has been a strong demand to gain a deeper understanding of the impact of efficient carbon coating over the lithiation and de-lithiation process of Si materials. Here, we report the first observation of the extended two-phase transformation of carbon-coated Si nanoparticles (Si/C) during electrochemical processes. The Si/C nanoparticles were prepared by sintering Si nanoparticles with polyvinylidene chloride precursor. The Si/C electrode underwent a two-phase transition during the first 20 cycles at 0.2C, but started to engage in solid solution reaction when the ordered compact carbon coating began to crack. Under higher current density conditions, the electrode was also found to be involved in solid solution reaction, which, however, was due to the overwhelming demand of kinetics property rather than the breaking of the carbon coating. In comparison, the Si/C composites prepared by sucrose possessed more disordered and porous carbon structures, and presented solid solution throughout the entire cycling process.

Keywords: Silicon, Carbon Coating, Electrochemical Behaviour, Lithium-ion Batteries, Anode

[*] Corresponding author. E-mail: gliu@lbl.gov.
[+]Shuo Zhou and Chen Fang should be considered joint first author.

TOC GRAPHICS

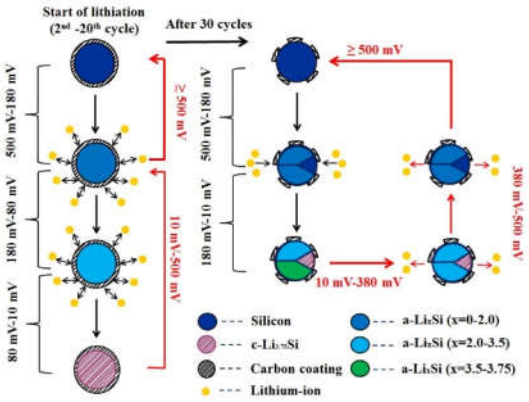

Introduction

Due to the high theoretical capacity (3579 mAh g^{-1}), low discharge potential (<0.5 V vs. Li/Li^+), abundant resource, and low cost, silicon (Si) material has been widely considered as one of most attractive candidates for next generation anode materials for lithium-ion batteries.[1,2] However, the commercial application of Si material is hindered by its poor conductivity and significant volume change that occurs during the formation of Li-Si alloy.[3,4] To address these challenges, carbon coatings[5-10] have been utilized to encapsulate Si materials (Si/C composite), simultaneously serving as conductive medium and buffering agent that could absorb the dramatic volume change.[11,12] For example, Fang et al.[13] reported a stable Si/C anode material where Si nanoparticles were inserted into hollow carbon nanofibers, delivering a capacity of 874 mA h g^{-1} at 0.8 A g^{-1} with a mass loading of 0.7 mg. Wu et al. [14] investigated the in situ polymerization of polyaniline (PANi) to attain conformal carbon structure to host Si materials. Such Si/C material with uniform coating layers on the surface of Si nanoparticles could provide superior performance of about 550 mA h g^{-1} after 5000 cycles at the current density of 6.0 A g^{-1} with a mass loading of 0.2–0.3 mg cm^{-2}. To understand the alloying mechanism of Si materials, the lithiation and de-lithiation processes of Si anodes have been extensively investigated by many in situ technologies, such as XRD,[15,16] TEM,[17,18] and NMR.[19,20]

However, there still remains a strong demand to gain deeper understanding of the impact of an efficient protective carbon coating on the lithiation and de-lithiation process of Si/C anode electrode.

Here, we report a compact and ordered carbon coating for Si electrodes prepared from polyvinylidene chloride (PVDC) precursor. The impact of this effective carbon coating over the solid-state transformation of Si electrode during electrochemical process is examined and discussed. To the best of our knowledge, this is the first report of extended two-phase transformation of carbon-coated Si nanoparticles (Si/C) during electrochemical processes.

Methods

Preparation of the Si/C composites

0.1 g Si particles (~50-70 nm, Nanostructured & Amorphous materials, Inc) and 0.8 g PVDC (polyvinylidene chloride, Sigma Aldrich Co.) were well dispersed in 20 mL tetrahydrofuran (THF, 99.9%, Sigma-Aldrich Co.) by being sonicated for 1 hour (Si). The mixture was then stirred for 12 hours at room temperature. After removal of volatile components under reduced pressure, the residual solid was collected and sintered at 800 °C for 2 hours (with a ramp rate of 1 °C min^{-1}) in argon atmosphere to obtain the final product (Si/C-P). The final mass ratio of silicon:carbon was 1:2 in Si/C-P sample. It was experimentally verified that the decomposition of PVDC precursors leads to a 1/4 carbon mass retention. Therefore, the Si:C ratio in final Si/C-P composite was controlled by the mass ratio of silicon and precursor. The Si/C-S sample was prepared in a similar manner with sucrose (Sigma-Aldrich). The silicon:sucrose mass ratio was 1:8 (1/8 carbon mass retention ratio for sucrose precursor), and the sample was sintered at 500 °C for 2 hours (with a ramp rate of 4 °C min^{-1}).The final mass ratio of silicon:carbon was 1:1 for Si/C-S sample.

Electrochemical evaluation

The Si/C composite particles, carbon black and PAA-Li binder were mixed at a mass ratio of 8:1:1 in deionized water to prepare the uniform slurry which was coated onto a copper foil as the working electrode. The electrolyte solution was purchased from BASF, which consists of 90% (w) of 1 M $LiPF_6$ solution (1 mol L^{-1}) in a mixture of ethylene carbonate (EC) and diethyl carbonate (DEC) (1:1 w/w) and 10% (w) fluoroethylene carbonate (FEC). Celgard 2400 separator was obtained from Celgard. The 2025 coin cells were used to assemble cells and the performances of these cells were evaluated with Maccor Series 4000 Battery Test system in a thermal chamber at 30 °C. The theoretical capacity of 1,000 mAh g^{-1} for Si/C composite materials was used to calculate charge/discharge currents. In the formation step, the cells were discharged and charged with one cycle in constant current-constant voltage (CC-CV) mode at 0.1C in a potential window of 0.01-2.0 V vs Li/Li^+. And then the cells were tested in constant current mode in a range of 0.01-1.0 V.

Materials characterization

Transmission electron microscopy (TEM, Tecnai) instrument from National Center for Electron Microscopy (NCEM) was performed at 200 kV to characterize the microstructure of the electrode. The cycled anode material was collected from the electrode that was washed by DEC in glove box. Fresh and cycled anode materials were dispersed in acetone and dropped on the copper grid (300 mesh). Scanning electron microscopy (JSM-7500F) was used at 10 kV to characterize the morphology of the electrode. In this test, the cycled electrode was washed by DEC in glove box and transferred by a sealed box into the instrument. Raman spectroscopy was performed to characterize the carbon structure of the Si/C composite. The Si/C composite material was compacted on the

clean glass slide and tested on an iHR 500 instrument with a He-Ne laser at 633 nm wavelength. Fourier Transforms Infrared Spectroscopy (FTIR) was conducted to characterize the structure of composite. The composite powder was mixed well with KBr powder and pressed into pellet. After dring at 40 °C overnight, the sample was measured on a Niclet-is50 instrument in the wavenumber range of 500-3500 cm^{-1} by 32 scans and the resolution setting of 4 cm^{-1}.

Results and Discussion

Si/C electrode with compact and ordered carbon coating was prepared with polyvinylidene chloride (Si/C-P electrode), and Si/C electrode with loose and porous carbon coating was made with sucrose (Si/C-S electrode) for comparison. The cells of the Si/C electrodes were cycled at 0.2C between 1.00 V and 0.01 V after a formation step at 0.1C. All the reported capacities in this paper are based on the total mass of Si/C composites. Figure 1a presents the cycling performance and Coulombic Efficiency (CE) of Si/C-P and Si/C-S. The initial Coulombic Efficiency (ICE) of Si/C-P (72.7%) is much higher than that of Si/C-S (56.1%). The compact carbon structure in Si/C-P sample can protect the silicon nanoparticles from direct exposure to the electrolyte, and thus lead to improved ICE.[21] After the formation step, the CE of Si/C-P electrode increases to above 99.0% after 10 cycles and to 99.5% after 20 cycles. On the other hand, the CE of Si/C-S electrode stays below 99.0%. This contrast demonstrates that Si/C-P electrode has enhanced kinetic properties comparing to Si/C-S electrode due to the presence of a compact carbon coating. Si/C-P electrode exhibits a specific charge capacity of 1219.6 mAh g^{-1} with the capacity retention of 98.1% after 20 cycles at 0.2C, which is higher than those of Si/C-S electrode, 692.7 mAh g^{-1} and 77.0 %, respectively. At the 25th cycle, the CE of Si/C-P electrode experiences a sharp decrease, dropping from 99.8 % to 98.6 %, which is rationalized as a consequence of the fracture of the carbon coating (observed in Figure 3c). After the fracture of the carbon coating, the CE of the Si/C-P electrode drops to about

98%, which is very similar to that of Si/C-S electrode. This significant drop of CE indicates that the Si/C-P electrode no longer has good kinetic properties after breakdown of carbon coating. During the 30-50th cycle, the Si/C-P electrode presents a gradually decreasing capacity from 1149.5 to 1078.0 mAh g^{-1}, and the capacity retention ratio of Si/C-P electrode during these 20 cycles is 93.8% (it is 98.1% retention for the first 20 cycles). These results indicate that the more compact carbon coating of the Si/C-P material helps to decrease interface reaction and increase cell life. In addition, after the break-down of the carbon coating on the Si/C-P sample, the interface stability of the Si/C-P sample begins to decay.

To better understand the electrochemical behavior of the Si/C-P electrode during lithiation and de-lithiation process, the voltage profiles of Si/C-P electrode from the 2nd-50th cycles are examined in Figure 1b. There is a major plateau at 0.43 V for the 2nd-20th de-lithiation curves, which disappears beyond the 30th cycle where the carbon coating is fractured. The disappearance of the voltage plateau at 0.43V indicates a significant bulk structure change during lithiation and de-lithiation processes due to the carbon coating fracturing. This is the first observation of the influence of compact and ordered carbon coating on bulk Si particle structure transformation during electrometrical process.

Figure 1c shows dQ/dV plots for Si/C-P electrode for 2nd-50th cycles. During the 2nd lithiation cycle, three different processes are observed. The first discharge process at ~250 mV is associated with the gradual lithiation of the a-Si to form $Li_{\sim 2.0}Si$, a structure that still presents extended Si networks and large Si-Si clusters.[22,23] The second process at ~80 mV is related to the further lithiation of $Li_{\sim 2.0}Si$ to $Li_{\sim 3.5}Si$. At this stage, large Si-Si clusters broke into smaller Si clusters and isolated Si anions. The third process at ~35 mV corresponds to the formation of the crystalline phase, c-$Li_{3.75}Si$, from a-Li_xSi.[15,24,25] The formation of c-$Li_{3.75}Si$ phase indicates that the outstanding

kinetic performance of compact carbon coating of the Si/C-P electrode leads to smooth and reversible lithiation/de-lithiation reaction. The third process is not observed beyond the 30th cycle. As for the de-lithiation process, there is a strong and sharp peak at ~430 mV for the 2nd-20th cycles, which is associated with the two-phase transition from c-$Li_{3.75}Si$ to Li_xSi (x=0-2.0).[19] In this case, the x value is approaching 0 to reflect the dominating two-phase transition from $Li_{3.75}Si$ to almost de-lithiated amorphous Si, with minor transition from Li_xSi to a-Si phase. However, beyond the 30th cycle, where the carbon coating is fractured, two broad peaks at ~280 mV and ~500 mV are observed instead (no sharp peak at ~430 mV), which is indicator of solid solution reaction.[26] This observation demonstrates that the formation of c-$Li_{3.75}Si$ is no longer the dominating process and that there is no direct transformation from c-$Li_{3.75}Si$ to amorphous Si particles. To be more specific, the two broad peaks are associated with the de-lithiation process of Li_xSi (x=3.5-3.75) to $Li_{\sim 3.5}Si$ (~280 mV) and $Li_{\sim 3.5}Si$ to $Li_{\sim 2.0}Si$ (~500 mV).[19] The two-phase transformation demands good conductivity and uniform evolution of the Si materials. The role of the compact and intact carbon coating is to improve the conductivity of Si materials and to promote the formation of the small Si clusters and isolated Si anions with uniformly dispersed silicon particles. These effects lead to enhanced alloying kinetics, which allows the Si/C-P electrode to continuously and completely generate c-$Li_{3.75}Si$ during lithiation process. Without effective carbon coating (fractured beyond 30th cycle as shown in Figure 3c), c-$Li_{3.75}Si$ can no longer be the dominating lithiation product and thus other less lithiated phases are formed, along with a decreased CE. The dQ/dV curves of Si/C-S sample (Figure S1) present a solid solution reaction from the 2nd cycle, indicating that carbon coating prepared by sucrose can hardly improve the alloying kinetics of the electrode to allow two-phase transitions. This is because the Si/C-S has a looser carbon coating, which cannot effectively confine the Si materials to realize good conductivity and uniform lithiation/de-lithiation

processes.

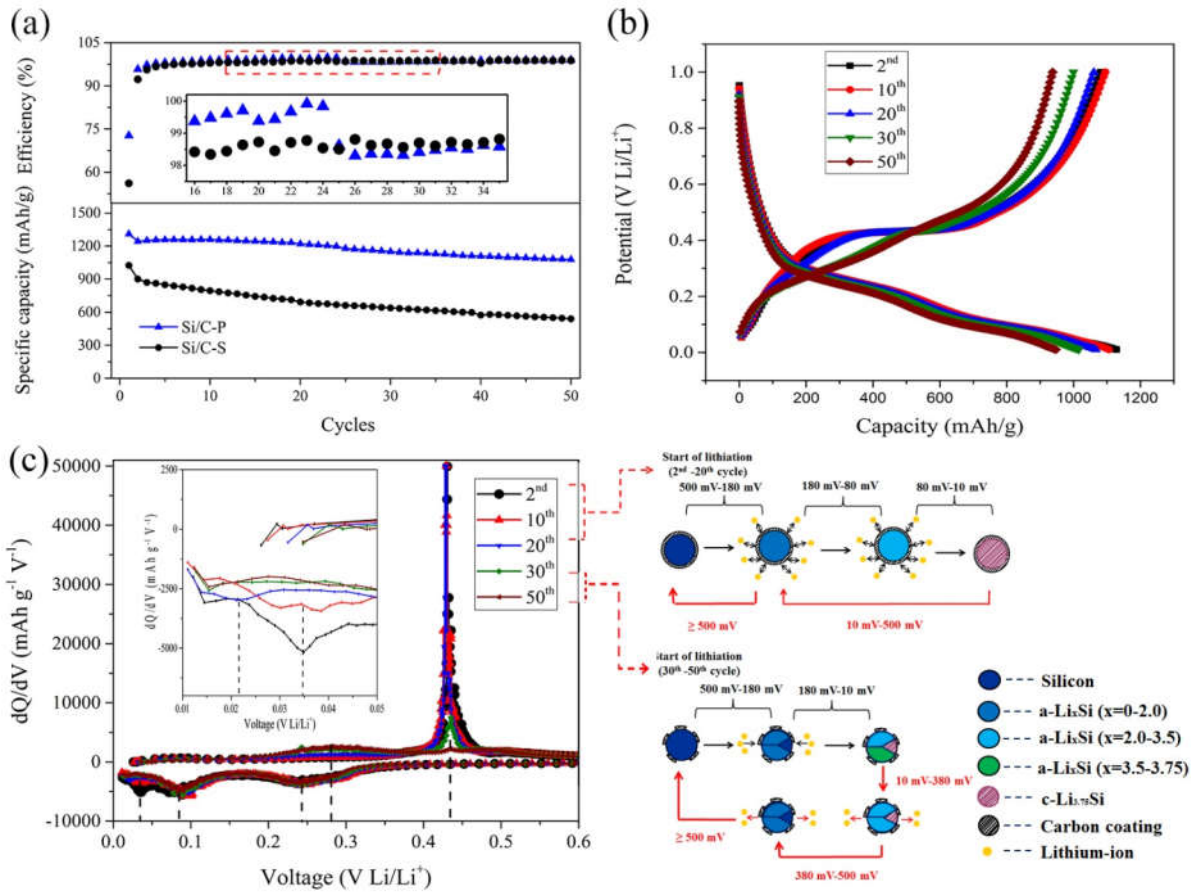

Figure 1. (a) Cycling performances and Columbic efficiencies of Si/C-P and Si/C-S electrodes at 0.2C, from 1.00V to 0.01V; (b) Galvanostatic discharge/charge profiles of Si/C-P electrode from 2nd to 50th cycles at 0.2C, from 1.00V to 0.01V; (c) Differential capacity vs. potential curves of Si/C-P electrode from 2nd to 50th cycles at 0.2C, from 1.00V to 0.01V (1C=1,000 mAh g^{-1}).

To understand how the carbon coating affects the electrochemical performance of the Si/C electrode at higher current densities, the Si/C-P electrode was discharged and charged in 5 cycles at various current densities. After the formation step, the Si/C-P electrode was cycled from 0.4C to 4C, and then back to 0.4C. As the rate increases (Figure 2a), the Si/C electrode shows a decreasing capacity,

from 1205.3 mAh g^{-1} at 0.4C to 926.1 mAh g^{-1} at 4C. When the rate is restored to 0.4C, the Si/C-P electrode shows a capacity of 1199.4 mAh g^{-1}, fully recovering its initial capacity. Also, the CE of the Si/C-P electrode exhibits a gradual increase without an outstanding drop. The recoverable specific capacity and increased CE indicates that the carbon coating remained intact under the high rate cycling process.

Figure 2b presents dQ/dV plots for Si/C-P electrode ranging from 0.4C to 4C. The two-phase transition of c-$Li_{3.75}Si$ and a-$Li_{\sim 2.0}Si$ can also be readily observed at 0.4C, indicating that the effective carbon coating in Si/C-P sample can provide sufficient kinetics capability to satisfy the demand of fast and uniform Li^+ migration and alloying reaction mediated by the carbon coating up to 0.4C. As the rate increases to 1C, the two-phase transition is still observed, although the intensity of the peak at ~430 mV drops dramatically, indicating that the formation of c-$Li_{3.75}Si$ becomes more difficult under 1C. When the rate reaches 2C and higher, the peak at 430 mV disappears entirely and the peaks at 280 mV and 500 mV emerge instead, indicating that the de-lithiation becomes a solid solution reaction. Remarkably, when the rate returns to 0.4C, the 430 mV peak re-appears and the Si/C-P material again presents the two-phase transition that is almost identical as the initial scenario at 0.4C. This result demonstrates the absence of the formation of the c-$Li_{3.75}Si$ for Si/C-P electrode at 2C and 4C is due to the overwhelming demand of the fast Li^+ migration and alloying kinetics for the electrode under high current density, rather than the break-down of the carbon coating.

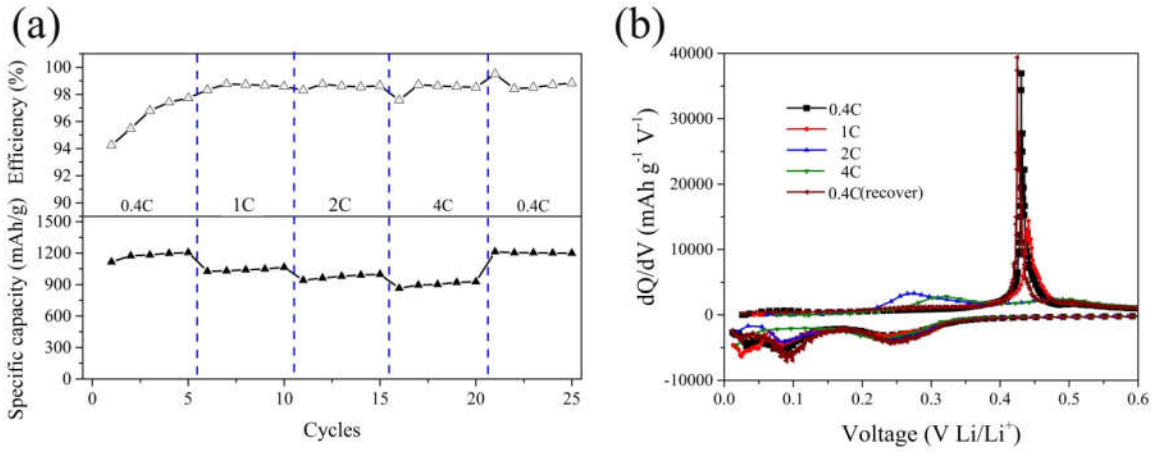

Figure. 2 (a) The rate capability and CE of Si/C-P electrode from 0.4C to 4C in the potential window of 1.00-0.01V; (b) The corresponding differential capacity vs. potential curves of Si/C-P electrode.

Scanning electron microscopy (SEM) was performed to investigate the morphology of the Si/C-P and Si/C-S materials before and after cycling. As shown in Figure 3a and d, both fresh Si/C-P and Si/C-S materials present Si nanoparticles well enclosed in a carbon matrix, forming micron-sized secondary particles. Figure 3b and c show that the Si/C-P materials still maintain the initial morphology of carbon coating after 10 cycles. After 50 cycles, the Si/C-P material presents cracked matrix and exposed Si particles (marked by red circle). These results indicate carbon coating has partially broken in the Si/C-P sample after 50th cycles. As shown in Figure 3e, a lot of broken carbon areas and agglomerated particles are observed in Si/C-S electrode after 50 cycles. To further understand the different morphologies of carbon coating by different precursors on the Si materials, TEM is used to analyze the Si and carbon interface structure. The nanostructures and the carbon/silicon structures in Si/C-P and Si/C-S samples before and after cycling were further characterized. As shown in Figure 3f and i, the silicon nanoparticles with a diameter of ~50 nm are well dispersed in compact carbon coating in fresh Si/C-P sample, while the carbon structure in fresh

Si/C-S sample is loose. In Figure 3g and h, the carbon coating maintains intact after 10 cycles in Si/C-P sample while the carbon edge becomes uneven with a few ~200 nm agglomerated particles (marked by red circle) observed after 50 cycles. From Figure 3j, some agglomerated particles attached with carbon fragments are observed for the Si/C-S electrode after 50 cycles. The SEM and TEM results confirm that the carbon structure in Si/C-P sample maintains compact and intact for the first 10 cycles. When the carbon coating began to crack (from 25th cycle), silicon particles in the broken carbon areas agglomerate to form large Si-Si cluster, resulting in the inhomogeneity of the Si/C structure. Such a change poses a negative influence on the alloying kinetics of the Si/C-P electrode due to the extra difficulties for Li^+ ion migration caused by the broken carbon coating. The TEM and SEM images described above provide direct support for the argument that effective carbon coating is essential for the good kinetic performance of Si/C-P. This explanation is consistent with the electrochemical observation that the Si/C-P electrode with intact and compact carbon coating could maintain the two-phase transition between 2nd and 20th cycle, but the carbon coating fracture that occurs beyond 25th cycle leads to a solid solution reaction. The breakdown of the compact carbon coating renders the carbon structure of Si/C-P composite looser and more porous, which can no longer allow two-phase transition. On the other hand, the Si/C-S electrode engages in solid solution reaction throughout the entire cycling process, indicating that Si/C-S has looser and more porous carbon structures than Si/C-P.

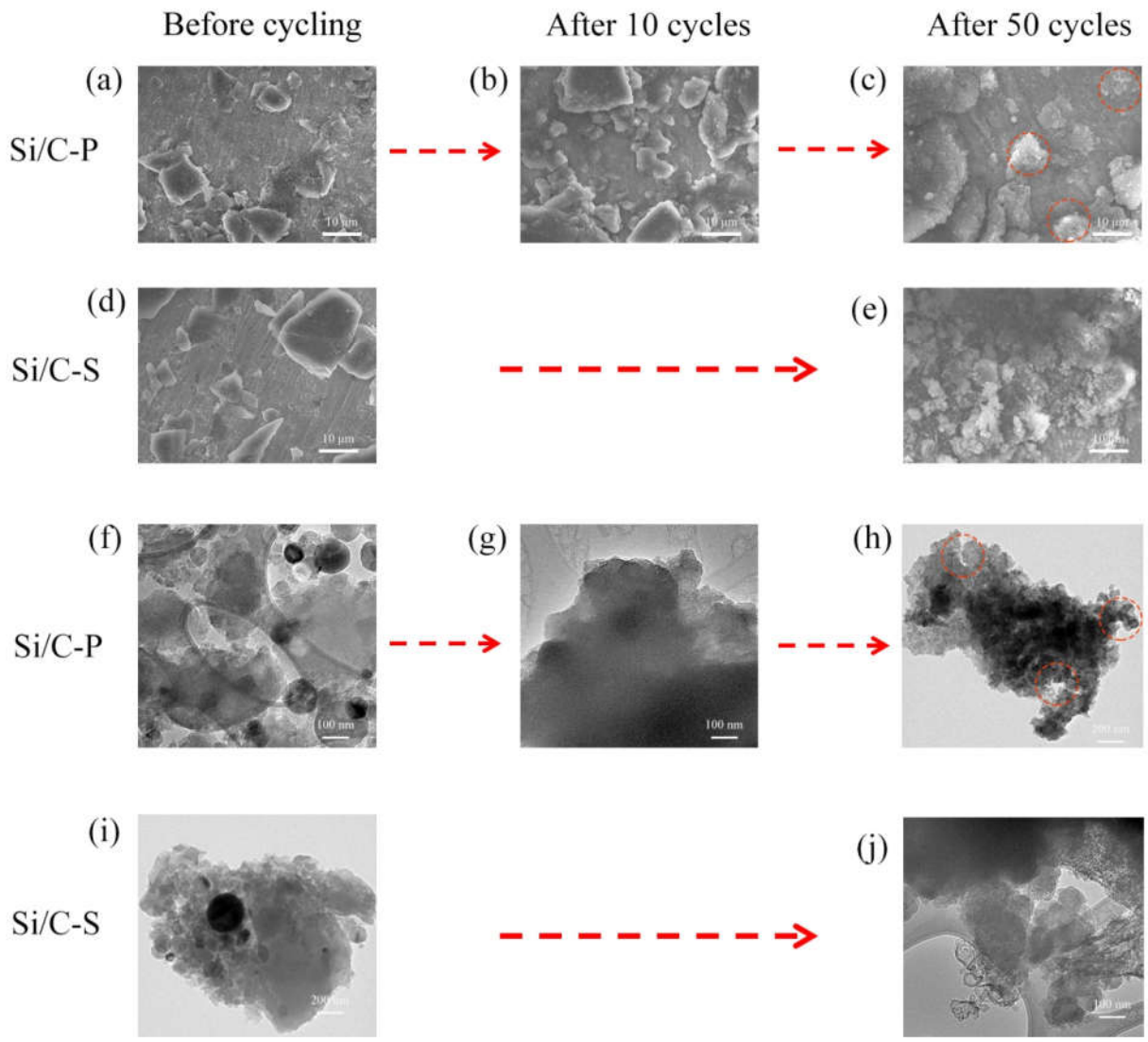

Figure 3. SEM images of the Si/C-P electrodes (a) fresh, (b) after 10 cycles, (c) after 50 cycles and Si/C-S electrode (d) fresh, (e) after 50 cycles at a current density of 0.2C. TEM images of the Si/C-P electrode (f) fresh, (g) after 10 cycles, (h) after 50 cycles and Si/C-S electrode (i) fresh, after (j) 50 cycles at a current density of 0.2C.

FTIR and Raman spectroscopy were performed to retrieve carbon bonding information of Si/C-S and Si/C-P samples. As shown in Figure 4a, only the C-C bond at 1250 cm^{-1} is observed for the Si/C-S sample, while there are two strong characteristic peaks at 2300 cm^{-1} and 1589 cm^{-1} for the

Si/C-P sample, which correspond to -C=C=C- and -C=C- bonds, respectively. These unsaturated carbon chains tend to undergo chain–chain cross-linking reaction, readily yielding ordered and compact sp^2-sp^3 hybrid carbon structures.[27,28] Also, the existence of the unsaturated carbon-carbon bonds can improve the conductivity of the Si/C composite. The compact and ordered carbon structure in Si/C-P sample was confirmed by the Raman spectra (Figure 4b). Both Si/C-P and Si/C-S samples exhibit two bands for carbon structure: the first at 1331 cm^{-1}, a D band, which is associated with disordered carbon structure, and the second at 1584 cm^{-1}, a G band, which is associated to ordered carbon structure.[29,30] The ratio of the G to D band intensities (I_G /I_D) of the Si/C-P sample is relatively high at 2.02, comparing to that of Si/C-S at 0.92. This contrast supports the conclusion that Si/C-P composite possesses a more ordered and compact carbon coating structure than Si/C-S composite.

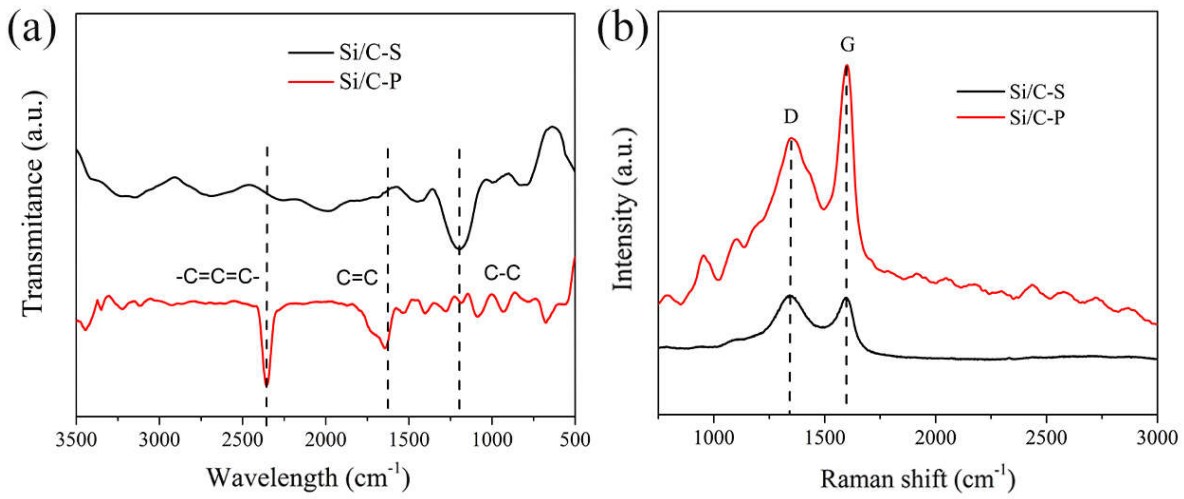

Figure. 4 (a) The FTIR spectra of Si/C-P and Si/C-S materials; (b) Raman spectra of Si/C-P and Si/C-S materials.

Conclusions

A compact and ordered carbon coating has been prepared from PVDC to encapsulate silicon nanoparticles. The Si/C-P electrode shows excellent electrochemical performance and improved CE, which reached above 99% only after 10 cycles. When the carbon coating was intact, there was a two-phase transition in Si/C-P electrode during lithiation and de-lithiation process. The carbon coating in Si/C-P electrode began to crack at 25th cycle, resulting in the decreased CE and eliminated formation of c-$Li_{3.75}Si$ (solid solution reaction). In addition, as the current density increased, the c-$Li_{3.75}Si$ formation became more challenging. When the rate increased to 2C, the electrode underwent a solid solution reaction, which was a result of the limited kinetic properties of the electrode rather than the fracture of carbon coating. The Si/C-S sample prepared by sucrose presented a loose carbon structure where only solid solution reaction happened during cycling process at 0.2C. These results indicate that a compact and ordered carbon coating can improve the Li^+ migration efficiency and help maintain the integrity of the electrode, which facilitates the two-phase transition during discharge and charge process.

Conflict of Interest

The authors declare that there are no conflict of interests.

Acknowledgments

This work is funded by the Assistant Secretary for Energy Efficiency, Vehicle Technologies Office of the U.S. Department of Energy, under the Si Consortium Program. Electron microscopy experiments are conducted at the National Centre for Electron Microscopy (NCEM) and the Molecular Foundry located at Lawrence Berkeley National Laboratory was supported by the

Director, Office of Science, Office of Basic Energy Sciences, of the U.S. Department of Energy under Contract No. DE-AC02-05CH11231.

References

1. Li J-Y, Xu Q, Li G, Yin Y-X, Wan L-J, Guo Y-G. Research progress regarding Si-based anode materials towards practical application in high energy density Li-ion batteries. *Mater Chem Front.* 2017;1(9):1691-1708.
2. Zuo X, Zhu J, Müller-Buschbaum P, Cheng Y-J. Silicon based lithium-ion battery anodes: A chronicle perspective review. *Nano Energy.* 2017;31:113-143.
3. Ryu J, Chen T, Bok T, et al. Mechanical mismatch-driven rippling in carbon-coated silicon sheets for stress-resilient battery anodes. *Nat Commun.* 2018;9(1):2924.
4. Higgins TM, Park S-H, King PJ, et al. A commercial conducting polymer as both binder and conductive additive for silicon nanoparticle-based lithium-ion battery negative Electrodes. *ACS Nano.* 2016;10(3):3702-3713.
5. Tatsuo U, Kenji F, Hongyu W, Nikolay D, Takashi I, Masaki Y. Novel Anode Material for Lithium-ion Batteries: Carbon-Coated Silicon Prepared by Thermal Vapor Decomposition. *Chem Lett.* 2001;30(11):1186-1187.
6. Yoshio M, Wang H, Fukuda K, Umeno T, Dimov N, Ogumi Z. Carbon-Coated Si as a Lithium-Ion Battery Anode Material. *J Electrochem Soc.* 2002;149(12):A1598-A1603.
7. Ng S-H, Wang J, Wexler D, Konstantinov K, Guo Z-P, Liu H-K. Highly Reversible Lithium Storage in Spheroidal Carbon-Coated Silicon Nanocomposites as Anodes for Lithium-Ion Batteries. *Angew Chem Int Ed.* 2006;45(41):6896-6899.
8. Kim MK, Shin WH, Jeong HM. Protective carbon-coated silicon nanoparticles with graphene buffer layers for high performance anodes in lithium-ion batteries. *Appl Surf Sci.* 2019;467-468:926-931.
9. Fang G, Deng X, Zou J, Zeng X. Amorphous/ordered dual carbon coated silicon nanoparticles as anode to enhance cycle performance in lithium ion batteries. *Electrochim Acta.* 2019;295:498-506.
10. Kim B, Ahn J, Oh Y, et al. Highly porous carbon-coated silicon nanoparticles with canyon-like surfaces as a high-performance anode material for Li-ion batteries. *J Mater Chem A.* 2018;6(7):3028-3037.
11. Wang M, Xia Y, Wang X, et al. Silicon oxycarbide/carbon nanohybrids with tiny silicon oxycarbide particles embedded in free carbon matrix based on photoactive dental methacrylates. *ACS Appl Mater Interfaces.* 2016;8(22):13982-13992.
12. Wang M-S, Song W-L, Wang J, Fan L-Z. Highly uniform silicon nanoparticle/porous carbon nanofiber hybrids towards free-standing high-performance anodes for lithium-ion batteries. *Carbon.* 2015;82:337-345.
13. Fang S, Shen L, Tong Z, Zheng H, Zhang F, Zhang X. Si nanoparticles encapsulated in elastic hollow carbon fibres for Li-ion battery anodes with high structural stability. *Nanoscale.* 2015;7(16):7409-7414.
14. Wu H, Yu G, Pan L, et al. Stable Li-ion battery anodes by in-situ polymerization of conducting hydrogel to conformally coat silicon nanoparticles. *Nat Commun.* 2013;4:1943.
15. Li J, Dahn J. An in situ X-ray diffraction study of the reaction of Li with crystalline Si. *J Electrochem Soc.* 2007;154(3):A156-A161.
16. Misra S, Liu N, Nelson J, Hong SS, Cui Y, Toney MF. In situ X-ray diffraction studies of (de) lithiation mechanism in silicon nanowire anodes. *ACS Nano.* 2012;6(6):5465-5473.
17. McDowell MT, Lee SW, Harris JT, et al. In situ TEM of two-phase lithiation of amorphous silicon nanospheres. *Nano Lett.* 2013;13(2):758-764.
18. Liu XH, Zhong L, Huang S, Mao SX, Zhu T, Huang JY. Size-dependent fracture of silicon nanoparticles during lithiation. *ACS Nano.* 2012;6(2):1522-1531.

19. Ogata K, Salager E, Kerr C, et al. Revealing lithium–silicide phase transformations in nano-structured silicon-based lithium ion batteries via in situ NMR spectroscopy. *Nat Commun.* 2014;5:3217.
20. Bhattacharyya R, Key B, Chen H, Best AS, Hollenkamp AF, Grey CP. In situ NMR observation of the formation of metallic lithium microstructures in lithium batteries. *Nat Mater.* 2010;9(6):504.
21. Young BT, Heskett DR, Nguyen CC, Nie M, Woicik JC, Lucht BL. Hard X-ray photoelectron spectroscopy (HAXPES) investigation of the silicon solid electrolyte interphase (SEI) in lithium-ion batteries. *ACS Appl Mater Interfaces.* 2015;7(36):20004-20011.
22. Key B, Morcrette M, Tarascon J-M, Grey CP. Pair distribution function analysis and solid state NMR studies of silicon electrodes for lithium ion batteries: understanding the (de) lithiation mechanisms. *J Am Chem Soc.* 2010;133(3):503-512.
23. Liu XH, Liu Y, Kushima A, et al. In situ TEM experiments of electrochemical lithiation and delithiation of individual nanostructures. *Adv Energy Mater.* 2012;2(7):722-741.
24. McDowell MT, Ryu I, Lee SW, Wang C, Nix WD, Cui Y. Studying the kinetics of crystalline silicon nanoparticle lithiation with in situ transmission electron microscopy. *Adv Mater.* 2012;24(45):6034-6041.
25. Liu XH, Zhang LQ, Zhong L, et al. Ultrafast electrochemical lithiation of individual Si nanowire anodes. *Nano Lett.* 2011;11(6):2251-2258.
26. Zamfir MR, Nguyen HT, Moyen E, Lee YH, Pribat D. Silicon nanowires for Li-based battery anodes: a review. *J Mater Chem A.* 2013;1(34):9566-9586.
27. Kijima M, Fujiya D, Oda T, Ito M. Efficient thermal conversion of polyyne-type conjugated polymers to nano-structured porous carbon materials. *J Therm Anal Calorim.* 2005;81(3):549-554.
28. Casari C, Bassi AL, Ravagnan L, et al. Chemical and thermal stability of carbyne-like structures in cluster-assembled carbon films. *Phys Rev B.* 2004;69(7):075422.
29. Dresselhaus MS, Jorio A, Hofmann M, Dresselhaus G, Saito R. Perspectives on carbon nanotubes and graphene Raman spectroscopy. *Nano Lett.* 2010;10(3):751-758.
30. Pawlyta M, Rouzaud J-N, Duber S. Raman microspectroscopy characterization of carbon blacks: spectral analysis and structural information. *Carbon.* 2015;84:479-490.